Current effects on higher harmonic waves

De-zhi Ning, Hong-xing Lin, Bin Teng
Department of Hydraulic Engineering, Dalian University of Technology, Dalian, 116024,China
e-mail: dzning@dlut.edu.cn, sunwind920@126.com, bteng@dlut.edu.cn

INTRODUCTION

The problem of waves propagating over a submerged obstacle has been widely investigated during the past decades. Higher bound and free harmonic waves are generated in the process of wave transformation above the submerged obstacle. As the important issues, the physics of harmonics generation and the nonlinear interaction among these harmonics were studied by many researchers, such as Grue (1992), Brossard and Chagdali (2001), Liu et al. (2009), Teng et al.(2010) and Ning et al. (2012). Actually, waves and currents generally coexist and their interactions play important roles in most of the ocean dynamic processes. Although numerous works on wave-current interactions, such as Thomas (1981), Zaman et al.(2008) and Yoon & Liu(1989), have been conducted, the analysis of current effects on the higher harmonics scattering by a submerged body is still relatively scarce.

In this abstract, the monochromatic wave over a submerged obstacle in the presence of uniform current is investigated using a fully nonlinear numerical scheme based on a 2D boundary element method (BEM). The phase-locked and free higher harmonic modes downstream the structure are decomposed by means of a two-point method, and their characteristics under the influence of current are further studied.

NUMERICAL MODEL

For wave overtopping a submerged obstacle in the presence of a uniform current as shown in Fig. 1, a 2D Cartesian coordinate system *oxz* is defined with the origin *o* in the plane of the undisturbed free surface, x=0 is at the left end of the domain, z is positive upwards. Fluid is assumed to be ideal, so that the potential flow theory can be used inside the fluid domain Ω. Due to the presence of uniform current U_0, the total velocity potential can be described to consist of component related to the current xU_0 and the rest part of potential $\varphi(x, z, t)$. Both the total velocity potential and φ satisfy the Laplace equation.

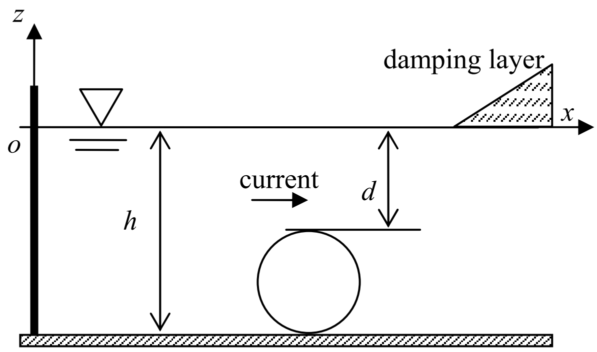

Fig.1 Sketch of the problem

On the instantaneous free surface, both the fully nonlinear kinematic and dynamic boundary conditions are satisfied and the mixed Eulerian-Lagrangian method is used to advance the time marching. On the bottom boundary, the rigid and impermeable condition is imposed. On the inflow boundary S_I, the fluid motion is generated by prescribing the second-order Stokes wave velocity. Due to the current effect, the input velocity potential can be written as follows

$$\varphi_I = \frac{gA_e}{\omega - kU_0}\frac{\cosh k(z+h)}{\cosh kh}\sin(kx-\omega t) + \frac{3}{8}A_e^2(\omega - kU_0)\frac{\cosh 2k(z+h)}{\sinh^4 kh}\sin 2(kx-\omega t) \qquad (1)$$

where ω is angular frequency, h is the static water depth, A_e is a parameter related to the wave amplitude in the presence of current. Based on the conservation of wave action (Bretherton & Garrett ,1968), it satisfies the following relation

$$A_e = A_0\sqrt{\frac{\omega - kU_0}{\omega}\frac{C_{g0}}{C_g}} \qquad (2)$$

in which A_0 and C_{g0} mean the wave amplitude and wave group velocity in quiescent water.

Towards the end of the computational domain, an artificial damping beach is applied on the free surface so that the wave energy is gradually dissipated in the direction of wave propagation (Ning et al., 2009).

By using the second Green's theorem, the prescribed boundary value problem can be transformed to the following boundary integral equation:

$$C(p)\varphi(p) = \int_{\Gamma} (\varphi(q)\frac{\partial G(p,q)}{\partial n} - G(p,q)\frac{\partial \varphi(q)}{\partial n})d\Gamma \tag{3}$$

where p and q are source and field points, and C is the solid angle which can be conveniently and economically computed by an indirect method in the present study. Γ is liquid domain boundary including free surface boundary and solid boundary. G is a simple Green function written as follows:

$$G(p,q) = \frac{1}{2\pi}(\ln r_1 + \ln r_2) \tag{4}$$

where $r_1 = \sqrt{(x-x_0)^2 + (z-z_0)^2}$,

$r_2 = \sqrt{(x-x_0)^2 + (z+z_0+2\mathrm{h})^2}$.

Then the boundary surface is discretized with a number of three-node line elements. The geometry of each element is represented by the quadratic shape functions, thus the entire curved boundary can be approximated by a number of higher-order elements. Within the boundary elements, physical variables are also interpolated by the same shape functions, i.e. the elements are isoparametric.

Since the discretized integral equation is always variant in time, all the boundary surfaces are regridded and updated at each time step using the mixed Eulerian-Lagrangian scheme and 4th-order Runga-Kutta approach. Once the Eq. (3) is solved, we can obtain the time series of surface elevation at any position.

When wave-current pass the submerged obstacle, higher harmonics generated by nonlinear wave-wave and wave-current interactions in the shallow water over the bar will leave the obstacle leeward as free waves. So the surface elevation at any point x in the lee side of the submerged body can be written as

$$\begin{aligned}\eta(t,x) = &\sum_{n=1}^{\infty} a_F^{(n)} \cos(k_n x - n\omega t + \psi_n(x)) \\ &+ \sum_{n=2}^{\infty} a_L^{(n)} \cos(n(kx - \omega t + \psi_1(x)))\end{aligned} \tag{5}$$

where $a_F^{(n)}$ are the amplitudes of the free transmitted waves with frequencies of integer times of the incident wave frequency, $a_L^{(n)}$ are the amplitudes of the nth-order phase-locked waves, $\psi_1(x)$ is the initial phase angle of the fundamental wave and $\psi_n(x)$ ($n \geq 2$) the nth harmonic free waves, k and k_n are the wave number of the fundamental waves and the nth harmonic free waves, and satisfy the following dispersion relations

$$(\omega - kU_0)^2 = gk \tanh kh \tag{6}$$

and

$$(n\omega - kU_0)^2 = gk_n \tanh k_n h,\ n = 2,3,\mathrm{L} \tag{7}$$

respectively. The fundamental wave amplitude, as well as the higher free and locked wave amplitudes, is obtained from the time histories of the surface elevation. The Fourier transform is introduced as follows

$$\eta_n(x) = \frac{1}{T}\int_0^T \eta(x,t)e^{-inwt}dt = A_n(x) + iB_n(x) \tag{8}$$

where $A_n(x)$ and $B_n(x)$ are the corresponding real and imaginary components, respectively. Then the two-point method (Grue, 1992, Teng et al., 2010) is used in the Eq.(8) and the unknowns in in Eq.(5) can be obtained.

NUMERICAL RESULTS

As a validation of the present model, the proposed numerical model is used to compute the combined wave-current field parameter in a domain with flat bottom, in which the input parameters static water depth h=0.6m, angular frequency ω=5.42rad/s, wave height H_0=0.06m are considered. The length of the corresponding computational domain is taken as 10λ($\lambda=2\pi/k$ denotes wave length), meshed with 200×10 cells in x and z directions after convergent tests, in which the last 1.5λ is used as the damping layer. Figs.2 and 3 show the comparisons of wave height and wave length in the presence of different current with other published numerical and experimental data, respectively. In the figure, the symbol C_0 represents the current-free wave celerity. From the figures, it can be seen that a good match of the numerical results with experimental data is observed.

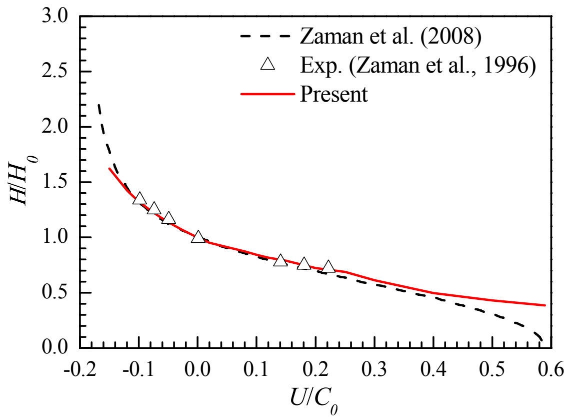

Fig.2 Comparisons of the wave height obtained by the present numerical model with Zaman et al.(2008) and experimental data (Zaman and Togashi, 1996).

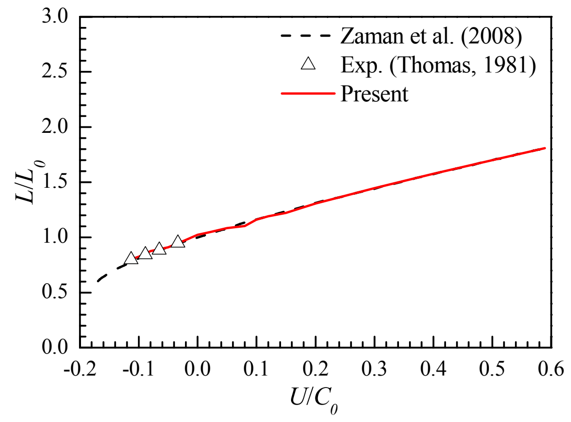

Fig.3 Comparisons of the wavelength obtained by the present numerical model with Zaman et al.(2008) and experimental data (Thomas, 1981).

To testify the two-point method for separating higher free harmonics from scattering waves, another case for monochromic wave propagating a submerged horizontal cylinder in quiescent water is considered as shown in Fig.1. Parameters including static water depth h=0.45m, cylinder radius R=0.1m, submerged depth d=0.1m are chosen. Fig.4 shows the distribution of the dimensionless fundamental and second-harmonic free wave amplitudes ($A_F^{(n)}/A_0$) with incident wave amplitude A_0. The comparisons between the present numerical results and experimental data (Grue, 1992) are also given here. From the figure, it can be seen that there are good agreements between numerical solutions and experimental data. The fundamental wave amplitude is always very close to the input one A_0, while the second-harmonic free amplitude is increased with the increasing of input wave amplitude A_0, and then reaches a maximum value at a critical input-amplitude.

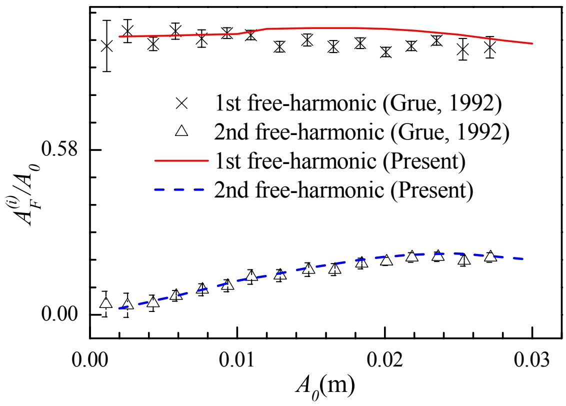

(a) wave period T=0.95s

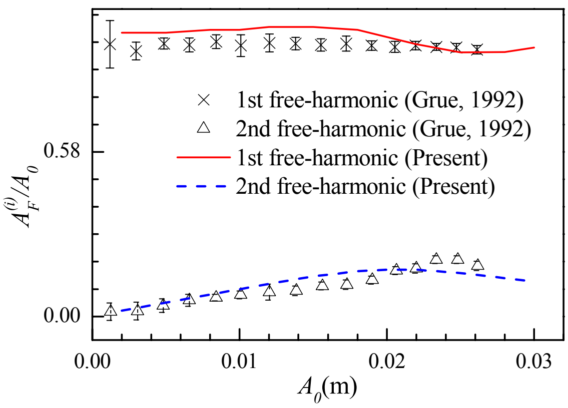

(b) wave period $T=0.82s$

Fig.4 Distribution of fundamental and 2nd-order free harmonic wave amplitudes with amplitude A_0.

Keeping the same wave parameters as those in Fig.4(a), three currents (i.e., U_0/C_{g0}=0, ±0.1) are introduced to the proposed numerical model. Fig.5 gives the distribution of the dimensionless fundamental, second- and third-harmonic free wave amplitudes with incident wave amplitude A_0. It can be seen that the portion of higher free harmonics becomes larger on the opposing current than that on zero current, but vice verse on the following current. Due to wave-current interactions, the maximum value of dimensionless higher free harmonic amplitude is upstream shifted for the opposing current relative to that for zero current. On the contrary, it is downstream shifted for the following current, as shown in Fig.5(b).

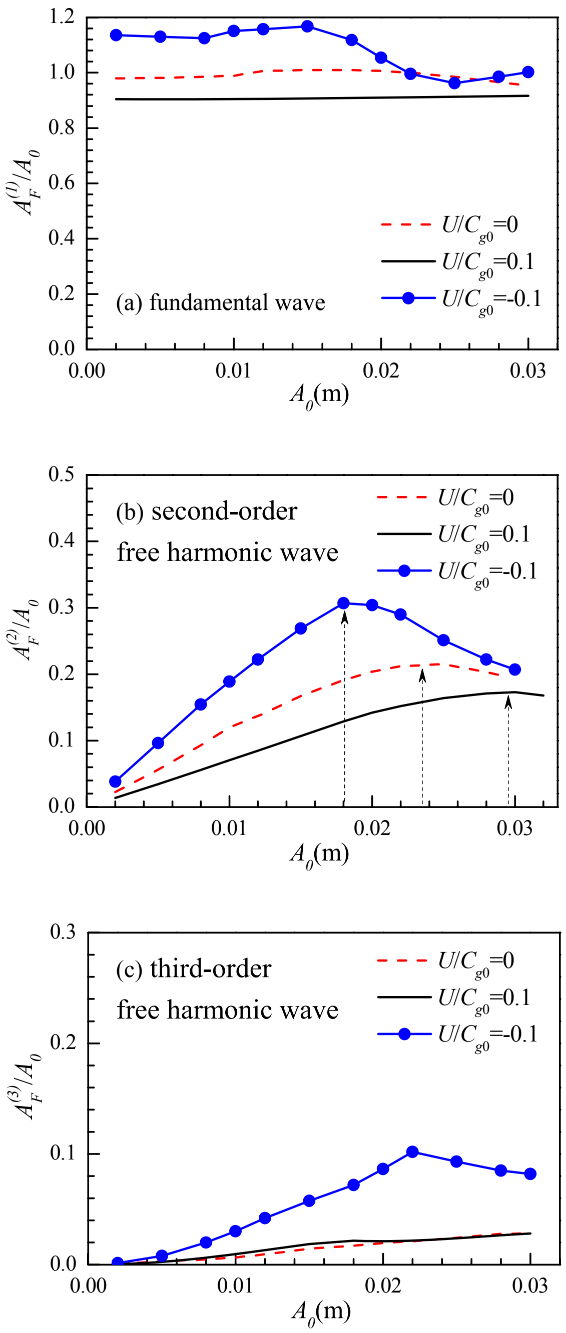

Fig.5 Distribution of harmonic amplitudes with A_0.

Numerical experiments of the effect of current velocity and input angular frequency on the higher harmonics are also carried out. The details will be shown in the workshop.

CONCLUSIONS

The phenomenon of wave propagation over a submerged obstacle in the presence of uniform current is examined by a powerful numerical model. The higher free harmonics are separated from the transmitted waves by using a two-point method. Good agreements of numerical results with the other published data are shown. The influence of the current on the characteristics of higher free harmonics are investigated.

ACKNOWLEDGEMENTS

The authors gratefully acknowledge the financial support from China NSFC (Grant Nos. 51179028, 51222902, 51221961).

REFERENCES

[1] Bretherton, FP and Garrett GJR (1968). "Wavetrains in inhomogeneous moving media." *Proceedings of the Royal Society of London*, 302, pp: 529-554.

[2] Brossard J and Chagdali M (2009). "Experimental investigation of the harmonic generation by waves over a submerged plate." *Coastal Engineering*, 42, pp: 277-290.

[3] Grue J (1992). "Nonlinear water waves at a submerged obstacle or bottom topography." *Journal of Fluid Mechanics*, 244, pp. 455-476

[4] Liu C R, Huang Z H, Tan S K(2009). "Nonlinear scattering of non-breaking waves by a submerged horizontal plate: Experiments and simulations" *Ocean Engineering*, 36, pp: 1332-1345.

[5] Ning D, Teng B, Zang J and Liu S(2009). "A fully nonlinear numerical model for focused wave groups." *Proceedings of 23rd IWWWFB*, Jeju, Korea

[6] Ning D, Zhuo X, Chen L and Teng B(2012). "Nonlinear numerical investigation on higher harmonics at lee side of a submerged bar." *Abstract and applied analysis*，doi: 10.1155/2012/214897

[7]Thomas G P(1981). "Wave-current interactions: an experimental and numerical study. Part 1. Linear waves. "*Journal of Fluid Mechanics*, 110, pp. 457-474.

[8] Teng B, Chen L, Ning D and Bai W(2010). "Study on the higher harmonic waves over a submerged bar." *Proceedings of 25th IWWWFB*, Harbin, China.

[9] Yoon S B and Liu PLF(1989). "Interactions of currents and weakly nonlinear water waves in shallow water." *Journal of fluid mechanics*, 250, pp:397-419.

[10] Zaman M H and Togashi H (1996). " Experimental study on interaction among waves, currents and bottom topography." *Proceedings of the Civil Engineering in the Ocean*, pp:49-54.

[11] Zaman M H, Togashi H and Baddour RE (2008). "Deformation of monochromatic water wave trains propagating over a submerged obstacle in the presence of uniform currents." *Ocean Engineering*, 35, pp:823-833.